Ab Initio Analysis of Monomers and Dimers of Trialkylphosphine Oxides: Structural and Thermodynamic Stability

THACIANA MALASPINA,[1] LUCIANO T. COSTA,[1] EUDES E. FILETI[2]

[1]*Instituto de Química, Universidade de São Paulo, São Paulo, SP, CP 26077, CEP 05513–970*

[2]*CCNH, Universidade Federal do ABC, Santo André, SP, CEP 09210–270*

Received 15 February 2008; accepted 19 March 2008
Published online 14 August 2008 in Wiley InterScience (www.interscience.wiley.com).
DOI 10.1002/qua.21754

ABSTRACT: Structural and thermodynamic stabilities of monomers and dimers of trialkylphosphine oxides (TRPO) were studied using quantum chemistry calculations. Density functional theory calculations were carried out and the structures of four TRPO have been determined: TMPO (methyl; R = CH_3), TEPO (ethyl; R = CH_3CH_2), TBPO (*n*-butyl; R = $CH_3(CH_2)_3$), and TOPO (*n*-octyl; R = $CH_3(CH_2)_7$). TRPO homodimers were investigated considering two isomeric possibilities for each dimer. Relative binding energies and the enthalpic and entropic contributions to the Gibbs free energy were calculated for all dimers. The formation of dimers from the individual monomeric TRPO species as a function of temperature was also analyzed. Int J Quantum Chem 109: 250–258, 2009

Key words: phosphine oxides; ab initio; structure; dimers; thermodynamic stability

1. Introduction

Trialkylphosphine oxides (TRPO) are chemical compounds of prime interest for industrial applications [1–9] as well as in organic chemistry [10–23]. In fact, TRPO are widely used in solvent extraction, a primary technology employed for the separation of transuranics and hazardous metal ions from waste solutions [1–9]. The use of TRPO has the advantage of the low cost of the TRPO reagents [9] and their proved extraction efficiency for several actinide and lanthanide elements in spite of the great affinity of phosphine oxide moieties for nitric acid, which promotes a competition of HNO_3 with the metal ions for extraction [11].

More recently tri-*n*-octylphosphine oxide (TOPO) and tri-*n*-butylphosphine oxide (TBPO), has been importantly used in the synthetic preparation of nanocrystals [16–19, 24–30], working as a capping ligand for quantum dots (e.g., CdSe quantum dots). In these cases, it stabilizes the nanoparticles in organic solvents preventing an irreversible aggregation of the nanocrystals [19, 30]. An interesting study on perturbation of the photolumines-

Correspondence to: E. Fileti; e-mail: fileti@ufabc.edu.br

Contract grant sponsors: FAPESP, CNPq.

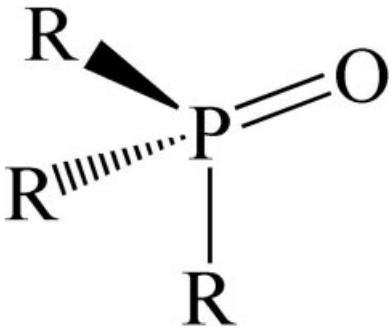

FIGURE 1. General structure of the phosphine oxides ($R_3P{=}O$).

cence of bulk CdSe demonstrate that at low concentrations TOPO acts like a labile base, enhancing the photoluminescence intensity upon adsorption [19]. At higher concentrations, stronger binding with Lewis acidic character was observed, represented by quenching of photoluminescence. This abrupt change in photoluminescence signature can be correlated with solution aggregate formation, identified through ^{31}P NMR and IR spectral measurements [19]. In this case, the characterization of the structural properties of the surfactants can be usefully employed to explain this phenomenon. To our knowledge very few computational studies on these systems have been performed. In fact, some theoretical studies on TMPO [31] and H_3PO [32], have been performed, but no systematic study of the structural, electric, and vibrational properties of the larger TRPO, as TBPO and TOPO, as well as the TRPO dimers. Therefore, we present a DFT study of the structural and vibrational properties of the most used TRPO and its corresponding possible dimeric forms.

2. Methodology

Fully optimized equilibrium geometry of each trialkylphosphine oxide (TRPO, general structure $R_3P{=}O$, see Fig. 1.) was obtained using density functional theory DFT (B3LYP).

The structures of four isolated TRPO have been determined: TMPO (methyl; R = CH_3), TEPO (ethyl; R = CH_3CH_2), TBPO (*n*-butyl; R = $CH_3(CH_2)_3$), and TOPO (*n*-octyl; R = $CH_3(CH_2)_7$). First, we have performed a benchmark to establish the minimum number of functions in the basis set necessary to converge the properties related to P═O bond using eight different basis sets. The structures of TRPO dimers were also investigated and their relative binding energies were evaluated using the same theoretical level of calculation used for the isolated molecule. For all TRPO structures, monomers and dimers, harmonic vibrational frequencies were calculated in order to ensure that the structures are in fact minima of the potential energy surface. As can be seen in Section 3.1, we have made use of the different basis sets to describe different sites in the molecule (locally dense basis set approximation). A larger basis set was used to describe the P atom as well as its first neighbors, and as shown in our benchmark, it overestimates the electronic binding energy in only 0.4 kcal/mol in the case of TMPO dimer. The effect of basis set superposition error (BSSE) on the calculated binding energies was examined by using the counterpoise method [33] for the TMPO, TEPO, and TBPO dimers. For these dimers, the results have shown that BSSE was lower than 0.5 kcal/mol and we believe that this value can be also used as good estimate for TOPO dimer. As the dimers are weakly bonded complexes, the applicability of DFT must be investigated. In order to investigate the quality of our B3LYP [34, 35] calculations, coupled-cluster [36] calculations were performed at the CCSD(T) and full-fourth-order perturbation theory (MP4) [37] levels, as well as a new model of functional [38] was employed to describe the binding energy of the TMPO dimer. Gaussian 03 program [39] was used in all calculations. The ChemCraft program [40] served as a graphics interface, allowing the visualization of the vibrational modes, the IR spectra, and the analysis of others properties.

3. Results

3.1. THE P═O BOND

Theoretical and experimental studies have characterized the P═O bond as polar, stronger, and shorter than conventional double bonds [15]. The correct theoretical description of the P═O bond requires the use of the polarization functions, due to the charge differences at phosphorus and oxygen atoms [41, 42]. Thus, we have investigated the minimum number of polarization functions necessary to characterize the related properties to P═O bond. In this case, we have performed a series of calculations with systematic increasing of the basis set size to the trimethylphosphine (TMPO) oxide monomer.

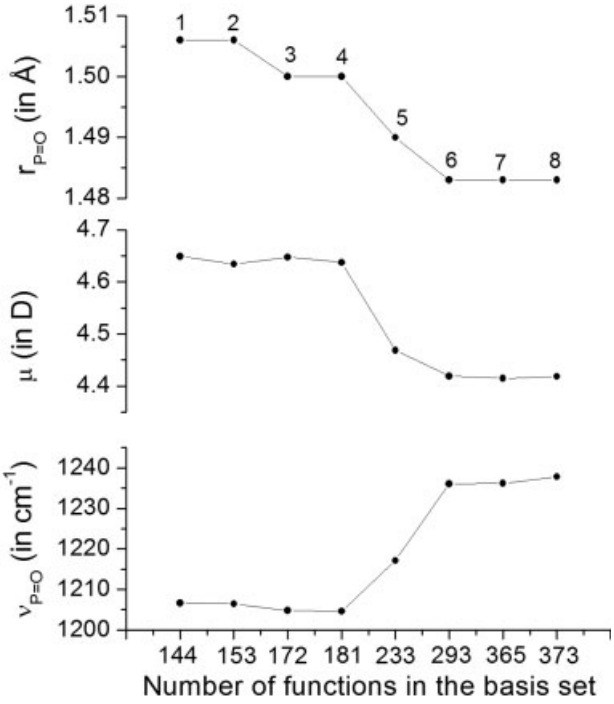

FIGURE 2. Convergence of the property with increase of the basis set size. At the top the P═O bond distance in Å, at middle the dipole moment in D and at the bottom the frequency of the $\nu_{P═O}$ stretching mode in cm^{-1}. 1. 6-31+G(d,p); 2. 6-31++G(d,p); 3. 6-311+G(d,p); 4. 6-311++G(d,p); 5. 6-311++G(2d,2p); 6. 6-311++G(3df,2p); 7. 6-311++G(3df,3pd); 8. 6-311++G(3d2f,2p). The relative CPU time from 1 to 8 is 1/1.3/1.8/3.0/13.5/16.8/28.7/33.4.

Figure 2 shows that adding one diffuse function (from 1 to 2 and from 3 to 4) the results are not improved, indicating no dependence on this type of functions. On the other hand, best results are obtained with the increase of the number of functions describing the valence orbitals (from 1 to 3 and from 2 to 4). However, converged values are obtained only adding polarization function (from 4 to 8). Overall eight basis sets were used in this analysis and converged values were only obtained from the 6-311++G(3df,2p) basis set, as it can be observed in Figure 2.

The experimental value for the P═O bond at TMPO is 1.476 Å[15] while our result shows a converged value of 1.483 Å, giving a good agreement with. For the dipole moment we have found a value of 4.42 D while the experimental value is 4.29 D [15]. For the frequency of the $\nu_{P═O}$ stretching mode we have found a non scaled value of 1236 cm^{-1}, while the experiment shows a fundamental frequency of 1163 cm^{-1} [15].

For the other monomers (TEPO, TBPO, and TOPO) the use of the 6-311++G(3df,2p) basis set in all atoms makes the calculations computationally unfeasible. To overcome this problem we have attributed the 6-311++G(3df,2p) basis set to P, O atoms and to three C atoms bonded to P atom. For the other atoms (C and H from alkyl chain) we have used the 6-31+G(d,p) basis set. Because of the computational cost in the frequency calculations of the TOPO dimers, we used the 3-21G basis set on the alkyl atoms to obtain the thermochemical corrections. Important to say that this systematic study was not made before.

3.2. STABILITY AND STRUCTURAL ANALYSIS

We have studied nine TRPO monomers: the single structure of the TMPO molecule (C_{3V} symmetry), two isomers of the TEPO molecule (C_3 and C_S symmetries), three isomers of the TBPO molecule (two of C_3 and one of C_S symmetries) and three isomers of the TOPO molecule (two of C_3 and one of C_S symmetries), as shown in Figure 3. We should point out that the isomers considered here are related only to the possible conformations for *n*-alkyl group, i. e., we are not considering species with *iso*, *sec* or *terc* chains.

Figure 3 shows all the systems considered here and below we discuss the main structural parameters for these optimized molecules. The calculated P═O and P—C distances for TMPO are 1.483 and 1.810 Å, respectively, in good agreement when compared with the experimental values of 1.476 and 1.809 Å [39]. The C—P—O and C—P—C angles are 113.6° and 105.0° while the experimental values are 114.4° and 104.1°, respectively [43], in good agreement. For other molecules all these values are very similar. The larger difference was found to the P═O and P—C distances increase to 1.487 and 1.831 Å, respectively in the case of the TEPO. From TEPO molecule these values practically do not change, except for the P—C distance in the S shape TBPO that presented a major value of 1.841 Å. No experimental results were found to TEPO, TBPO, and TOPO. The R parameter is the length of the chain alkyl, measured from P atom to last C atom of the chain and provides an estimative of the size of the molecule.

Table I presents the value for total (E) and relative energies (ΔE). All values including zero-point vibrations correction.

We can observe that the Y shape is systematically more stable than other forms. In the TEPO

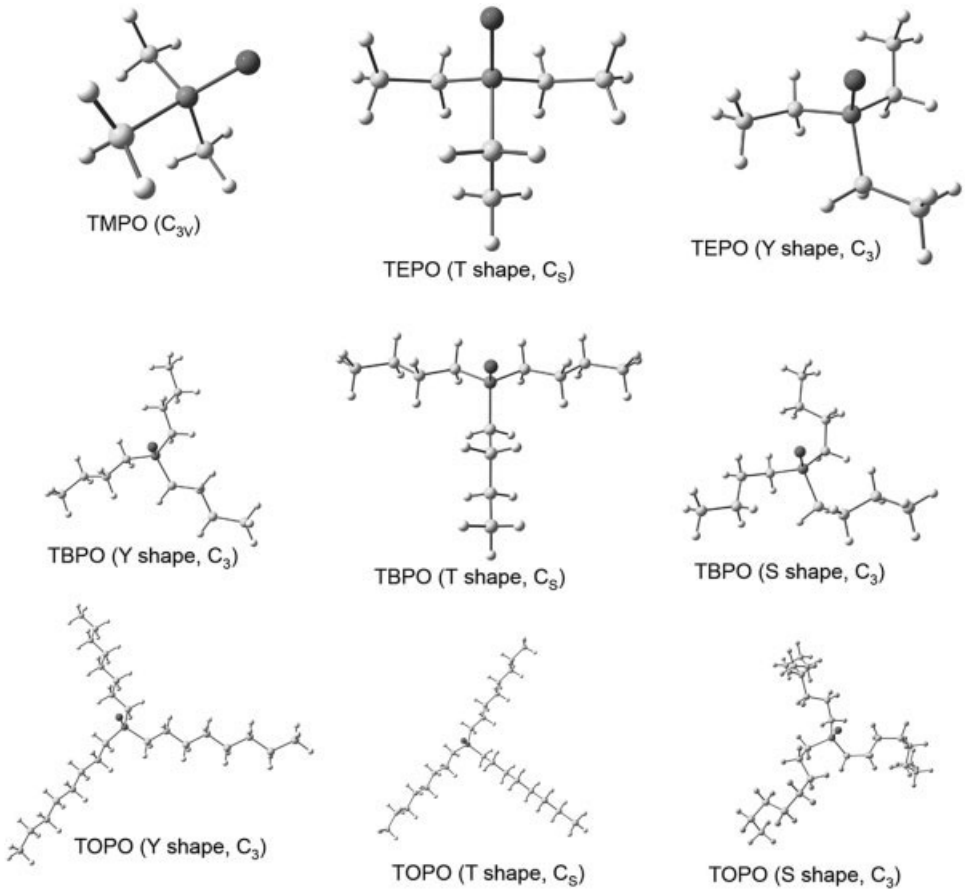

FIGURE 3. Optimized structures of the TRPO.

TABLE I

Total energies (in a.u.), relative energy (in kcal/mol), dipole moment (in debye), and rotational constants (in MHz) for TRPO optimized molecules.

R	E	ΔE	μ	I_A	I_B	I_C
Methyl	−536.4807103	0.0	4.42	3739.3	3739.3	3556.0
Ethyl (Y)	−654.3962850	0.0	4.04	1573.1	1573.1	1000.8
Ethyl (T)	−654.3957133	0.4	4.27	1982.6	1319.3	1040.6
n-Butyl (Y)	−890.2819038	0.0	3.90	371.2	371.2	198.9
n-Butyl (T)	−890.2793083	1.6	3.81	518.0	297.9	203.4
n-Butyl (S)	−890.2745931	4.6	3.51	446.2	446.2	248.8
n-Octyl (Y)	−1362.0505520	0.0	3.80	63.5	63.5	32.3
n-Octyl (T)	−1362.0479571	1.6	3.72	96.8	49.4	33.3
n-Octyl (S)	−1362.0219859	18.0	3.18	90.0	88.9	49.2

Y and S shape has C_3 symmetry while T shape has C_S symmetry. In all values for the energies are included the zero point vibrations correction.

case, the Y shape is only 0.4 kcal/mol more stable than the T shape. For the TBPO, the Y shape is more stable by 1.6 kcal/mol in relation to T shape and 4.6 kcal/mol in relation to S shape. For the TOPO the Y shape is more stable by 1.6 kcal/mol in relation to T shape and 18.0 kcal/mol in relation to S shape. The dipole moment is also presented at Table I and we can observe that larger the alkyl group the minor is the dipole moment. For instance, to Y shape we have 4.42, 4.27, 3.90, and 3.80 D for TMPO, TEPO, TBPO, and TOPO, respectively. The rotational constants are shown and as expected the larger the molecule the minor is the rotational constant.

Charge distributions of the monomers are examined in terms of the natural bond orbital (NBO) analysis based [44, 45]. In recent years, the use of the NBO analysis has been widespread. Unlike most other partitioning schemes, the presence of diffuse functions in the basis set has a marginal effect on this method. As follows from NBO calculations, the charge on P atom increase from 1.90*e* when in TMPO to 1.95*e* when in TOPO. For the oxygen atom, the charge in TMPO is −1.11*e* and in TOPO −1.12*e*. These values corroborate the polar nature of the P═O bond. Although the charge on P atom increases from TMPO to TOPO, it was shown the dipole moment decreases with augment of alkyl group. This result can be justified by the larger charge distribution that occurs in TOPO where the polarization effect is more pronounced than in TMPO.

3.3. VIBRATIONAL ANALYSIS

In this section we analyse the vibrational spectra of the more stable isomers, i. e., all isomers at the Y shape.

Table II presents the frequencies of the most characteristic normal modes: nondegenerate $\nu_{P═O}$ stretching (*A* symmetry), doubly degenerate $\nu_{P—C}$ stretching and $\delta_{C—P—O}$ (both *E* symmetry), and nondegenerate $\delta_{C—P—C}$ bending (*A* symmetry). For the $\nu_{P═O}$ stretching we have found the same value for the frequency, 1217 cm^{-1} except to TMPO that presented a higher value, of 1236 cm^{-1}. Jensen [31] has found for this frequency a value of 1215 cm^{-1} at DFT/6-311G(d,p), however in light of the discussion of the section 3.2 this result can be overestimated by the absence of diffuse functions at the basis set. As mentioned before, this mode has fundamental frequency of 1163 cm^{-1}. For the $\nu_{P—C}$ stretching we have observed that the frequency increases with the alkyl chain size. TMPO and TOPO presented the lowest (640 cm^{-1}) and highest (683 cm^{-1}) value, respectively. In the case of $\delta_{C—P—O}$ bending a increase at the frequency is observed from TMPO (350 cm^{-1}) to TEPO (477 cm^{-1}) but for TOPO this tendency is broken and a value of 431 cm^{-1} was obtained. Experimental values were found only for TMPO and in these cases they are 699 and 317 cm^{-1} for $\nu_{P—C}$ stretching and $\delta_{C—P—O}$ bending, respectively. Finally the $\delta_{C—P—C}$ bending presented the the lowest (232 cm^{-1}) and highest (316 cm^{-1}) value for TMPO and TEPO, respectively. The experimental value for this fundamental frequency in TMPO is 249 cm^{-1} [15].

TABLE II

Frequencies (in cm^{-1}) for selected modes of the TRPO molecules for the more stable isomers (C_{3v} symmetry, shape Y).

R	$\nu_{P═O}$	$\nu_{P—C}$	$\delta_{C—P—O}$	$\delta_{C—P—C}$
TMPO	1236	640	350	232
TEPO (Y)	1217	675	444	316
TBPO (Y)	1217	678	477	275
TOPO (Y)	1217	683	431	235

3.4. TRPO DIMERS

3.4.1. Structure

IR measurements have provided evidences that phosphine oxides can form dimers in many solvents [30]. In a previous work, it has been argued that the interaction between TOPO molecules at the capping of a nanocrystal can alter the photoluminescence process. Thus we have considered interesting to study the stability of TRPO homodimers and to investigate what is the expected isomeric composition. We have analyzed two isomeric possibilities for each dimer, a "head-to-tail" (type I) and "head-to-head" (type II), see Figure 4.

All dimers are stable under harmonic vibrational frequency analysis, excepting the type 2 TMPO dimer that presented an imaginary frequency of −49 cm^{-1} and will not be considered in the next analysis. Table III presents the distances P···O between two monomers, the dipole moments and the rotational constants for the dimers.

In the case of type I dimers, TEPO and TOPO present the largest and lowest P···O distances, respectively, 3.949 and 3.832 Å. For type II dimers the

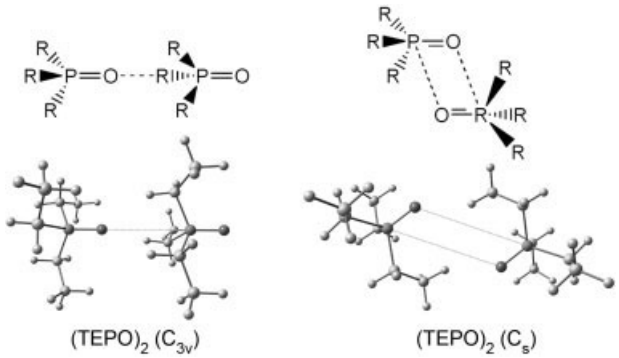

FIGURE 4. At top, the general scheme for the two isomers dimers of TRPO: the type I (head-to-tail) and the type II (head-to-head). At bottom, as 3D example, the optimized structures of the TEPO.

largest and lowest distances occurs to TBPO and TEPO, respectively, 5.276 and 5.134 Å. Upon complexation the combined dipole moment of the type I dimer has a larger value when compared with the corresponding of type II dimer. In the first case there is a large parallel component whereas in the latter there is a large anti-parallel component of the separate dipole moments as it can be seen in Figure 4. In the case of the TOPO the dipole moment for the type I and type II dimer are, respectively, 9.38 D and 0.60 D. In general the dipole for type I dimers are roughly double of dipole moment in their isolated corresponding and the dipole moment of type II dimers are very small. The rotational constants also are given and as expected the values increase from TMPO to TOPO.

TABLE III

Dipole moment (in debye), P· · ·O distances (in Å) and rotational constants (in MHz) for TRPO optimized dimers.

R	P· · ·O	μ	I_A	I_B	I_C
TMPO-I	3.902	10.31	1786.1	315.4	315.4
TEPO-I	3.949	9.65	500.4	193.2	193.2
TEPO-II	5.134	0.47	601.9	153.7	146.3
TBPO-I	3.939	9.38	99.6	85.5	85.5
TBPO-II	5.276	0.00	131.7	67.2	57.6
TOPO-I	3.832	9.16	24.5	24.5	16.2
TOPO-II	5.213	0.60	25.8	20.2	14.0

TABLE IV

Electronic binding energy for the TMPO using 6-311++G(3df,2p) basis set in all atoms.

Level	Generation	ΔE
CCSD(T)		−7.60
MP2		−7.67
MPWLYP1W	G	−4.69
PBE1PBE	H	−5.39
B97–2	H	−4.24
B3LYP	H	−4.49
BHandHLYP	H	−5.43
MPW1K	H	−5.08
MP3LYP	H	−5.44
B98	H	−5.13
B3PW91	H	−3.82
G96LYP	M	−1.54
BB95	M	−3.49
MPWB1K	HM	−5.79

The geometry was reoptimized in each level, except CCSD(T) for which we used the MP2 geometry. G, M, H, HM indicate the generation of the functional, see text. BSSE and zero point vibrations corrections are not included.

Vibrational analysis were performed for all dimers and we found that changes of the frequencies upon the dimerization are negligible being lesser than 5 cm^{-1} inclusive for ν_{PO} stretching.

3.4.2. Thermodynamic Stability

To evaluate the performance of B3LYP functional, we have performed calculations in CCSD(T) and full-fourth-order MP4 levels as well as used more modern functional, for instance MPWB1K, to determine the binding energy of TMPO dimer. The results for this analysis are shown at Table IV.

We can see that the CCSD(T) reference value is −7.60 kcal/mol while the MP2 value is −7.67 kcal/mol indicating that the role of electron correlation effects beyond MP2 is not very important in defining the relative strengths of the dimer. On the other side, the correlation effects are very important for describing properly the binding energy of the dimer. We have tested functional of all generation (G, GGA; H, hybrid, M, meta-GGA; and HM, hybrid-meta-GGA); see a recent review at reference [38]. At Table IV, we can find the values for all functionals used. These values are in a range from −1.54 kcal/mol (G96LYP) to −5.79 kcal/mol (MPWB1K), being the latter the best DFT value

TABLE V

Relative energies including correction to the difference in zero-point vibrations, enthalpies, entropy contribution and free energies (in kcal/mol) for all dimers of Figure 4.

Dimer	$\Delta(E+ZPE)$	ΔH	$-TS$	ΔG
TMPO-I	−3.96	−3.20	5.77	2.57
TEPO-I	−3.33	−2.42	8.14	5.72
TEPO-II	−1.39	−0.56	8.48	7.92
TBPO-I	−3.38	−2.44	8.72	6.28
TBPO-II	−2.30	−1.54	10.13	8.59
TOPO-I	−4.18	−4.29	13.90	9.61
TOPO-II	−2.15	−1.60	13.11	11.51

BSSE correction is not included. Gibbs free energy can be calculated from the individual Gibbs free energy for each isomer, $G = H - TS$, by explicitly considering the thermal corrections to the thermodynamic functions using the well-known statistical mechanical formulation for gas-phase molecules.39,46

among all functionals. B3LYP provides an energy of −4.49 kcal/mol, this value is 41% lower than reference value and 22% lower that the best DFT value. This scenario was also obtained in our preliminary tests for phosphine oxide dimer, $(PH_3)_2$, where all DFT energies are underestimated, at the least, by 15% for the best result. Since none functional can describe properly the binding energy of the dimer (our best value is 24% below the reference value). We have chosen the B3LYP functional for estimating the thermodynamic stability of the dimers, in view of the fact that this functional generally yields very good structures [38].

Table V presents the relative binding energies and the enthalpic and entropic contributions to Gibbs free energy. By the analysis of the relative potential energy we can observe that overall the dimers of type I are systematically more stable than dimers of type II.

The binding energy of type I TEPO and TOPO dimers were found as −3.33 and −4.18 kcal/mol, respectively. These results for type II dimers are −1.39 and −2.15 kcal/mol. Previous estimative using a macromodel molecular mechanics gives to type II TOPO dimer a value of −12.7 kcal/mol [19]. Because the entropic change of dimerization is always negative all enthalpy gain at the formation of dimer is cancelled. In this way the calculated Gibbs free energies are always positive at room temperature. As can seen at Table V the values varying from 2.57 kcal/mol to 11.51 kcal/mol for type I TMPO and type II TOPO dimers respectively. In case of type II TMPO dimer, the enthalpy in vacuum, −1.60 kcal/mol, is increased to 11.51 kcal/mol when corrected to entropy.

From Table VI we can also observe that the $\Delta\Delta G$ between type I and type II dimers are −2.21, −2.31, and −1.91 kcal/mol for TEPO, TBPO, and TOPO, respectively. Thus, a question to consider is the formation of the dimers from the individual monomeric TRPO species as a function of temperature. The $\Delta G°$(dimer) can be calculated at different temperatures from the binding energy of the TRPO dimer at 0 K by calculating the appropriate thermochemical corrections for the monomeric and the dimeric species. The calculated temperature variation of $\Delta G°(TRPO_2)$ and ln $K_{(TRPO2)}$ yield the data displayed in Figure 5. We can observe that $\Delta G°(TEPO_2)$, for instance, is predicted to become negative at temperatures below 100 K, thus leading to favorable cluster formation at these lower temperatures. According to our calculations, type I dimers are only stable for temperatures around 100 K, while type II dimers should only be stable around 40 K. These results clearly indicate that, at room temperature, the formation of both dimers is unlikely to occur. Using CCSD(T) as a reference, we observed that these values should be corrected by 40% (see Table IV), leading to larger temperatures. Even this way, dimers should only be stable around 150 K that is obviously not enough to warrant their observation at room temperature.

4. Conclusion

A DFT study of the structural, vibrational, and energetic properties of the most common TRPO

TABLE VI

Relative stability (kcal/mol) between the type I and type II dimers, considering the thermochemical contribution.

Dimer	$\Delta\Delta(E+ZPE)$	$\Delta\Delta G$
TEPO	−1.94	−2.21
TBPO	−1.08	−2.31
TOPO	−2.03	−1.91

Values at 1 atm and 298.15 K. BSSE corrections are not included.

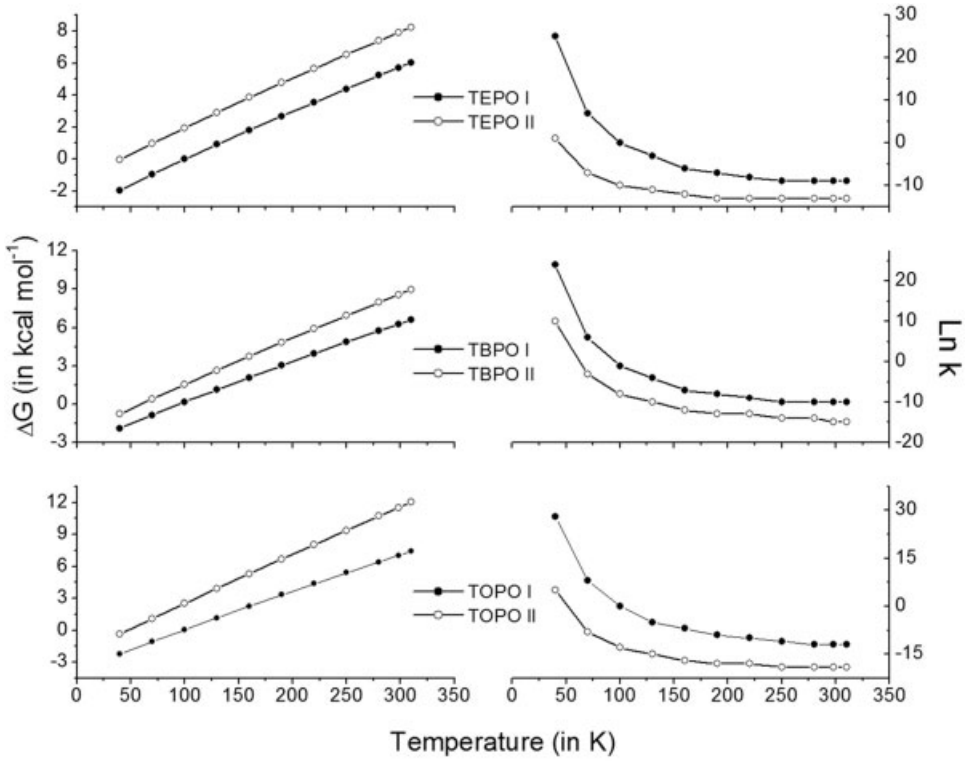

FIGURE 5. Temperature dependence of $\Delta G°$ and ln K of the TRPO dimers. I and II stands for the types of the dimers. The isomeric composition can be obtained from the equilibrium constant K for isomerization [39, 46], $\Delta G°(TRPO_2) = (RT \ln K$, where $\Delta G°(TRPO_2)$ is the difference between the gas phase standard Gibbs free energy of the two isomeric species. This difference is given at Table VI.

was presented. A systematic analysis of the basis set effects was performed and it was observed that converged values for P═O distance, dipole moment and ν_{PO} stretching frequency were obtained only from the 6-311++G(3df,2p) basis set. The structural analysis of the monomers of TRPO shows that the isomer with chains in Y shape is systematically more stable than other forms. In the case of TOPO, the Y shape is 1.6 and 18.0 kcal/mol more stable than the T and S shapes, respectively. It was observed that larger the alkyl group the minor is the dipole moment, is special to shape Y we have 4.42, 4.27, 3.90, and 3.80 D for TMPO, TEPO, TBPO, and TOPO, respectively.

The performance of the B3LYP was tested and compared with others functionals. For this evaluation, calculations in CCSD(T) and full-fourth-order MP4 levels were performed as well as used more modern functional to determine the binding energy of TMPO dimer. It was observed that MP2 level can provides reliable values for the binding energy. For other side, none of DFT functional can describe it properly, underestimating these values in 22% at the best case. B3LYP provides a binding energy of −4.49 kcal/mol. This value is 41% lower than reference value and 22% lower that the best DFT value. This scenario seems valid for all dimers of R_3P═O, inclusive to $(PH_3)_2$, for which all DFT energies are underestimated, at the least, by 15% for the best result, in preliminary tests.

For dimers case, two isomeric possibilities for each dimer were analyzed, a "head-to-tail" (type I) and "head-to-head" (type II) and was found that type I dimers are more stable that type II dimers. The binding energy estimative of TOPO dimers, for instance, were found being as −4,18 and −2.15 kcal/mol, for type I and type II dimers, respectively. The formation of the dimers from the individual monomeric TRPO species as a function of temperature was investigated and we found that $\Delta G°(TRPO_2)$, is predicted to become negative at temperatures below 100 K for type I dimers and below 40 K for type II dimer, evidencing the lesser stability of the later. Using CCSD(T) as a reference,

we observed that these values should be corrected by 40% (see Table IV), leading to larger temperatures. Even this way, dimers should only be stable around 150 K that is obviously not enough to warrant their observation at room temperature.

ACKNOWLEDGMENTS

The authors are thankful to Dr. Gustavo Dalpian and Dr. Roberto Rivelino for helpful suggestions.

References

1. Suresh, G.; Murali, M. S.; Mathur, J. N. Radiol Chim Acta 2003, 91, 127.
2. Xu, L.; Xiao, Y.; Li, D. J Chem Inf Comput Sci 1992, 32, 437.
3. Matsuyama, H.; Nakamura, K.; Miyake, Y.; Teramoto, M. Ind Eng Chem Res 1992, 31, 2103.
4. Shaibu, B. S.; Reddy, M. L. P.; Bhattacharyya, A.; Manchanda, V K. J Magn Magn Mater 2006, 301, 312.
5. Kim, Y. S.; In, G.; Choi, J. M. Bull Korean Chem Soc 2003, 24, 1495.
6. Paiva, A. P.; Malik, P. J Radioanal Nucl Chem 2004, 261, 485.
7. Reddy, M. L. P.; Ramamohan, T. R.; Sahu, S. K.; Chakravortty, V. Radiol chim Acta 2000, 88, 33.
8. Zhu, Y.; Jiao, R. Nucl Radiochem 1994, 108, 361.
9. Eccles, H. Solvent Extr Ion Exchange 2000, 18, 547.
10. Steinberger, H. U.; Ziemer, B.; Meisel, M. Acta Crystallogr C 2001, 57, 323.
11. Jiang, J.; Li, W.; Gao, H.; Wu, J. J Colloid Interface Sci 2003, 268, 208.
12. Liggieri, L.; Ravera, F.; Ferrari, M.; Passerone, A.; Miller, R. J Colloid Interface Sci 1997, 186, 46.
13. Liggieri, L.; Ravera, F.; Ferrari, M.; Passerone, A.; Miller, R. J Colloid Interface Sci 1997, 186, 40.
14. Prochaska, K.; Walczak, M.; Staszak, K. J Colloid Interface Sci 2002, 248, 143.
15. Gilheany, D. G. Chem Rev 1994, 94, 1339.
16. Yang, C. S.; Awschalom, D. D.; Stucky, G. D. Chem Mater 2001, 13, 594.
17. Green, M.; O'Brien, P. Chem Commun 2001, 1912.
18. Rabani, E. J. Chem Phys 2001, 115, 1493.
19. Lorenz, J. K.; Ellis, A. B. J Am Chem Soc 1998, 120, 10970.
20. Rakiewicz, E. F.; Peters, A. W.; Wormsbecher, R. F.; Sutovich, K. J.; Mueller, K. T. J Phys Chem B 1998, 102, 2890.
21. Green, M.; Allsop, N.; Wakefield, G.; Dobson, P. J.; Hutchison, J. L. J Mater Chem 2002, 12, 2671.
22. Jiang, J.; Krauss, T. D.; Brus, L. E. J Phys Chem B 2000, 104, 11936.
23. Wang, C.; Robertson, A.; Weiss, R. G. Langmuir 2003, 19, 1036.
24. Asami, H.; Abe, Y.; Ohtsu, T.; Kamiya, I.; Hara, M. J Phys Chem B 2003, 107, 12566.
25. Kim, B. S.; Islam, M. A.; Brus, L. E.; Herman, P. I. J Appl Phys 2001, 89, 8127.
26. Saponjic, Z. V.; Csencsits, R.; Rajh, T.; Dimitrijevic, N. M. Chem Mater 2003, 15, 4521.
27. Wu, D.; Kordesch, M. E.; van Patten, P. G. Chem Mater 2005, 17, 6436.
28. Wang, X. S.;Dykstra, T. E.; Salvador, M. R.; Manners, I.; Scholes, G. D.; Winnik, M. A. J Am Chem Soc 2004, 126, 7784.
29. Zou, S.; Hong, R.; Emrick, T.; Walker, G. C. Langmuir 2007, 23, 1612.
30. Liu, H.; Owen, J. S.; Alivisatos, A. P. J Am Chem Soc 2007, 129, 305.
31. Jensen, J. O. J Mol Struct (THEOCHEM) 2005, 723, 1.
32. Dobado, J. A.; García, H. M.; Molina, J.; Sundberg, M. R. Quantum Systems in Chemistry and Physics, Vol. 2; Kluwer Academic: Dordrecht, 2000.
33. Boys, S. F.; Bernardi, F. Mol Phys 1970, 19, 553.
34. Lee, C.; Yang, W.; Parr, R. G. Phys Rev B 1988, 37, 785.
35. Becke, A. D. Phys Rev A 1988, 38, 3098.
36. Raghavachari, K. Annu Rev Phys Chem 1991, 42, 615.
37. Bartlett, R. J. J Phys Chem 1989, 93, 1697.
38. Souza, F. S.; Fernandes, P. A.; Ramos, M .J. J Phys Chem A 2007, 111, 10439.
39. Frisch, M. J.; Trucks, G. W.; Schlegel, H. B.; Scuseria, G. E.; Robb, M. A.; Cheeseman, J. R.; Montgomery, J. A., Jr.; Vreven, T.; Kudin, K. N.; Burant, J. C.; Millam, J. M.; Iyengar, S. S.; Tomasi, J.; Barone, V.; Mennucci, B.; Cossi, M.; Scalmani, G.; Rega, N.; Petersson, G. A.; Nakatsuji, H.; Hada, M.; Ehara, M.; Toyota, K.; Fukuda, R.; Hasegawa, J.; Ishida, M.; Nakajima, T.; Honda, Y.; Kitao, O.; Nakai, H.; Klene, M.; Li, X.; Knox, J. E.; Hratchian, H. P.; Cross, J. B.; Bakken, V.; Adamo, C.; Jaramillo, J.; Gomperts, R.; Stratmann, R. E.; Yazyev, O.; Austin, A. J.; Cammi, R.; Pomelli, C.; Ochterski, J. W.; Ayala, P. Y.; Morokuma, K.; Voth, G. A.; Salvador, P.; Dannenberg, J. J.; Zakrzewski, V. G.; Dapprich, S.; Daniels, A. D.; Strain, M. C.; Farkas, O.; Malick, D. K.; Rabuck, A. D.; Raghavachari, K.; Foresman, J. B.; Ortiz, J. V.; Cui, Q.; Baboul, A. G.; Clifford, S.; Cioslowski, J.; Stefanov, B. B.; Liu, G.; Liashenko, A.; Piskorz, P.; Komaromi, I.; Martin, R. L.; Fox, D. J.; Keith, T.; Al-Laham, M. A.; Peng, C. Y.; Nanayakkara, A.; Challacombe, M.; Gill, P. M. W.; Johnson, B.; Chen, W.; Wong, M. W.; Gonzalez, C.; Pople, J. A. Gaussian 03, revision D. 01; Gaussian, Inc.: Wallingford, CT, 2004.
40. ChemCraft Program: Tool for treatment of chemical data. http://www.chemcraftprog.com. 2006.
41. Magnusson, E. J Am Chem Soc 1993, 115, 1051.
42. Magnusson, E. J Am Chem Soc 1990, 112, 7940.
43. Wilkins, C. J.; Hagen, K.; Hedberg, L.; Shen, Q.; Hedberg, K. J Am Chem Soc 1975, 97, 6352.
44. Foster, J. P.; Weinhold, F. J Am Chem Soc 1980, 102, 7211.
45. Reed, A. E.; Curtius, L. A.; Weinhold, F. Chem Rev 1988, 88, 889.
46. McQuarrie, D. A. Statistical Thermodynamics; Harper and Row: New York, 1973.